Achievement of Record β in the START Spherical Tokamak

M. Gryaznevich,[1] R. Akers,[1] P. G. Carolan,[1] N. J. Conway,[1] D. Gates,[1] A. R. Field,[1] T. C. Hender,[1] I. Jenkins,[1] R. Martin,[1] M. P. S. Nightingale,[1] C. Ribeiro,[1] D. C. Robinson,[1] A. Sykes,[1] M. Tournianski,[2] M. Valovič,[1] and M. J. Walsh[3]

[1]*UKAEA Fusion, Culham Science Centre, Abingdon, Oxon, OX14 3DB, United Kingdom**

[2]*University of Essex, Wivenhole Park, Colchester, United Kingdom*

[3]*Walsh Scientific Ltd., Abingdon, Oxon, OX14 2RT, United Kingdom*

(Received 17 November 1997)

Values of $\beta_T \geq 30\%$ have been achieved and sustained for several confinement times on the START spherical tokamak using additional heating provided by neutral beam injection. These values are more than twice the highest value previously obtained in a tokamak, and correspond to normalized β values of $\beta_N \geq 4$. In these shots values of $I_p > I_{\mathrm{rod}}$ (where I_{rod} is the current flowing in the central toroidal field rod) have been obtained, which are considered to be necessary for spherical tokamak power plant. The results are compared with ideal-MHD stability theory. [S0031-9007(98)05532-X]

PACS numbers: 52.55.Fa

A spherical tokamak (ST) is the low aspect ratio limit of the tokamak (aspect ratio $A = R/a$ is the ratio of the major to minor radii of the torus). Peng and Strickler in 1986 [1] summarized several advantages of the ST over the conventional tokamak. These advantages include simplicity of construction, lower magnetic field requirements, and improved plasma stability. Interest in this concept is growing rapidly and the potential for an eventual fusion power plant has recently been favorably reported [2]. The first experimental verification of many of these properties has been provided by START (small tight aspect ratio tokamak) at UKAEA Fusion, Culham [3,4].

The Troyon [5] and Culham [6] empirical scalings imply that the β achievable in a tokamak should be maximized by a combination of low aspect ratio and high plasma shaping (high elongation and triangularity), where β is the ratio of the plasma pressure to the pressure of the magnetic field required to contain the plasma. This dependence has been verified experimentally over a wide range of tokamaks [7,8], and indeed the previous highest value of β was achieved on the DIII-D tokamak which combines (relatively) low aspect ratio $A \sim 2.8$ and high elongation and triangularity. The highest value achieved in DIII-D is $\beta_T = 12.6\%$ [7], where $\beta_T = (2\mu_0/VB_0^2)\int p\,dV$ and B_0 is the vacuum toroidal magnetic field at the geometric center of the plasma.

The START device was built in 1990 to provide a first hot plasma test of the spherical tokamak concept. Details of the construction of the device and a summary of the operational features are given in [3]. In START, aspect ratios as low as $A \sim 1.2$ can be achieved, although the results described in this paper concern plasmas separated from the center column, having $A \sim 1.3$–1.45 ($R \sim 0.3$–0.37 m, $a \sim 0.22$–0.28 m). These double-null diverted START plasmas have a high plasma elongation ($\kappa \sim 1.7$–1.9) and triangularity ($\delta \sim 0.5$), without requiring fast vertical position control [4]. To investigate behavior under auxiliary heating, a 40 keV neutral beam injector has been loaned to Culham by the U.S. DOE and Oak Ridge National Laboratory. The results described here were obtained using tangential coinjection of hydrogen neutrals into deuterium target plasmas, and operation to date has been at energies $\leq$35 keV with injection power up to approximately 0.8 MW. The present layout of the START device is shown in Fig. 1, together with an equilibrium reconstruction of a high-β discharge #32993.

The first investigations of NBI heating into START, reported in [9], used an injection of about 0.5 MW of 30 keV hydrogen neutrals into hydrogen and deuterium plasmas and obtained $\beta_T \sim 11\%$, only slightly less than the DIII-D value, and the record value of the central $\beta_T(0) \sim 48\%$. These results from START are shown (open circles) in Fig. 2, together with an indication of other existing high tokamak β values. The "Troyon limit" of $\beta_N = 3.5$ found in conventional tokamaks [7] is indicated, where $\beta_N = \beta_T/(I_p/aB_T)$, (%, MA, m, T) is the normalized β. Although in these early auxiliary heated START discharges $\beta_N \leq 2.5$, the values of β_T are high because START can operate at very high normalized current $I_N = I_p/aB_T$ before q_{95} falls below the stability bound, i.e., has a high "shaping factor" $S = (I/aB)q_{95}$ due to the low aspect ratio, high elongation, and triangularity of the plasma [8].

Following these initial results, a range of improvements has been made to the START facility. In order to reduce first orbit losses of the beam ions it is necessary in START to operate at relatively high plasma current $I_p \geq 200$ kA. This imposes demands on both the volt seconds available from the central solenoid and the vertical field required to maintain the radial position of a high current, high pressure plasma. Recent improvements to the START solenoid and vertical field power supplies have addressed these. In addition, boronization and titanium gettering have reduced the impurity influxes, especially of oxygen, and the wall

 0031-9007/98/80(18)/3972(4)$15.00

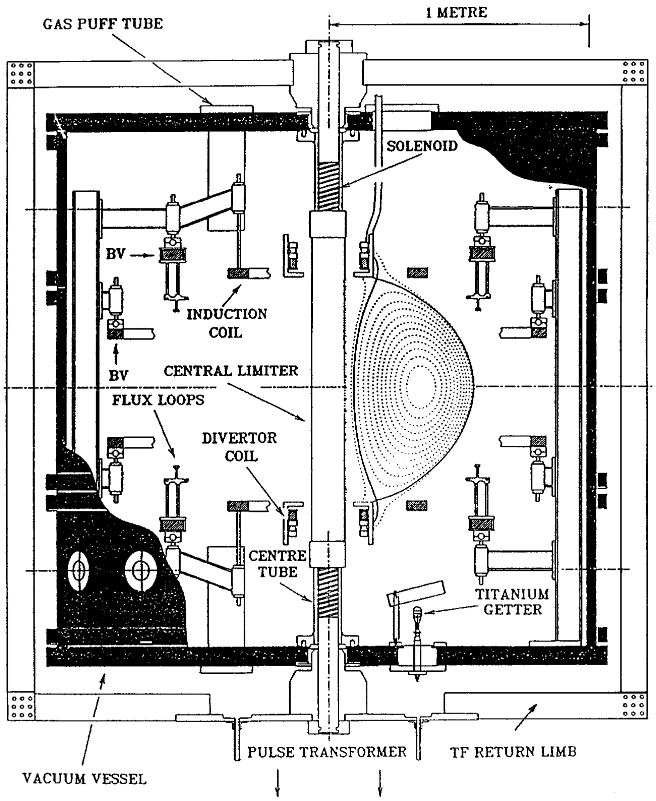

FIG. 1. Cross section of the START device (April, 1997) showing an equilibrium reconstruction of high-β shot #32993.

is further conditioned by helium glow discharge cleaning between shots.

As in other high-β_N experiments on DIII-D [8], TFTR [10], and JT60-U [11], operating regime optimization is very important on START. Optimization of the current ramp and density ramp is believed to be a key feature of the increase in shaping factor and normalized current of up to $I_N \sim 8$, (Fig. 2): the relatively broad current profile produces plasmas of high elongation and triangularity. This value of normalized current on START is substantially greater than the value $I_N \sim 3$ previously achieved in optimized conventional aspect ratio tokamaks [7]. A value of $I_p/I_{\rm rod}$ up to 1.2 has been obtained on START representing an important result in itself, as economic considerations for ST power plant designs suggest $I_p \geq I_{\rm rod}$ is necessary. As a result of these steps, $\beta_T > 30\%$ and $\beta_N > 4$ have been achieved (solid symbols in Fig. 2). Traces for several high-β shots are presented in Fig. 3.

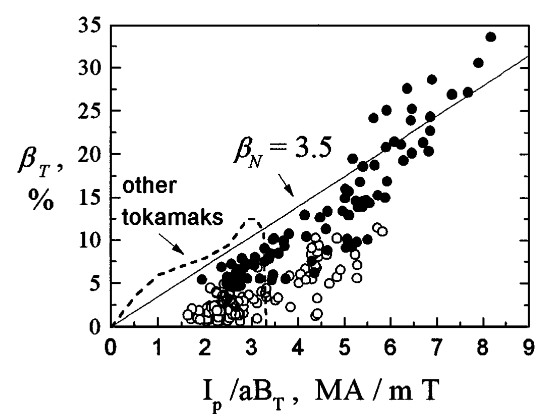

FIG. 2. β_T vs I_p/aB_T in START; high-β operation limits for other tokamaks are shown for comparison.

The β values were deduced from magnetic measurements and cross-checked with kinetic data. Equilibrium reconstruction using magnetic data (including the diamagnetic loop signal) was done with two independent codes TOPEOL (developed at Culham) and EFIT [12]. The electron temperature and density profiles were measured with a 30 point Thomson scattering diagnostic and the central ion temperature was obtained by multichord charge exchange spectroscopy [13]. Figure 4 presents Thomson scattering profiles in high-β discharge #32993 with maximum $\beta_T \sim 31\%$, $\beta_N \sim 3.9$. The high edge density gradient and very flat density profile, accompanied by a reduction of the scrape-off layer thickness, are typical features of high-β discharges on START. The plasma thermal energy, i.e., not including the fast ion component, at this time was estimated from kinetic measurements to be $W_T^{\rm kin} \sim 1.45 \pm 0.15$ kJ. The fast ion component was estimated from beam simulations [14] at 0.2–0.4 kJ, which makes the kinetic and magnetic values ($W_T^{\rm mag} \sim 1.77$ kJ) consistent.

Typical high-β shot traces are shown in Fig. 3: the record β_T shot #32998 with maximum $\beta_T \sim 34\%$ (Fig. 3.1); a high-β_N shot #33006 with $\beta_N \sim 4.6$ (Fig. 3.2); and a high-β_T, high-β_N shot #34237 in which the high-β value was sustained for several energy confinement times (Fig. 3.3). The plasma current was ramped up with a rate $dI_p/dt \sim 10$ MA/s [Figs. 3.1(a), 3.2(a), 3.3(a)] and programmed gas puffing was used to prevent the plasma current profile from becoming hollow, which is undesirable for neutral beam power absorption. As a result, the l_i value $[l_i = l_i(2) = (1/B_{\rm pa}^2) \int B_p^2\, dV$, where $B_{\rm pa} = \int B_p\, dl / \int dl]$ was kept ~0.7 throughout the shot. The toroidal field was decreased (allowing β to rise) by decreasing the central rod current, $I_{\rm rod}$ [Figs. 3(a)], typically from 0.3 to 0.15 T. In shot #34237 the central rod current was then kept constant for ~10 ms from the moment when I_p reached $I_{\rm rod}$, Fig. 3.3(a), which prevented q_{95} from decreasing and allowed the high-β plasma to remain for several energy confinement times ($\tau_E^{\rm exp} \leq 2$ ms and is close to the ITERH97 empirical scaling prediction). High-β_N values of $\beta_N \geq 4$ can be achieved on START at normalized current values I_N from 5 up to 8, Fig. 2; however, the highest β_N discharge with $\beta_N = 4.6$, #33006 (Fig. 3.2), had $I_N \sim 5.8$ and a higher q_{95} value ($q_{95} \sim 2.9$) compared with #32998 (Fig. 3.1), which had $q_{95} \sim 2.2$.

In these regimes, the density increases throughout the shot, Figs. 3.1(b), 3.2(b), 3.3(b), and this is the main

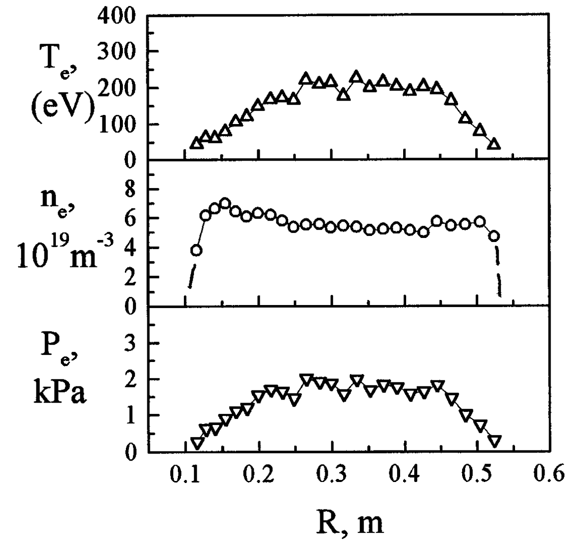

FIG. 4. Profiles of electron temperature, density, and pressure at time $t = 35$ ms in shot #32993 ($\beta_T \sim 31\%$, $\beta_N \sim 3.9$).

source of the pressure rise; however, density and temperature profiles become flatter after the beginning of the sawteeth, Fig. 4. The values of internal inductance of the highest β plasmas were found to be in a narrow range of $l_i \sim 0.6$–0.8 and the pressure profile was broad, with peakedness $p(0)/\langle p \rangle \leq 2$. Unlike DIII-D and JT60-U [8,11], the highest β_N values have been obtained on START using current ramp-up; however, the highest β_T values on DIII-D [8] were obtained at low l_i values, similar to those on START. At higher l_l values (l_l up to 1.6), obtained using a current ramp-down technique similar to DIII-D and JT60-U (with $dI_p/dt \sim -10$ MA/s), the highest β_N values obtained so far on START are below 3.5 and the predicted $\beta_N \sim 4l_i$ limit [8] has not been reached yet.

Analysis of Mirnov coil and SXR data shows that the MHD activity in high-β plasmas on START can be either an $m/n = 1/1$ slowly rotating mode, or coupled low-n Mirnov activity with $m/n = 2/1, 3/1$. In the highest β shots sawtooth activity usually replaces the low-n fluctuations and the sawtoothing stage continues until the current rapidly terminates, possibly due to contact with the divertor coils (see Fig. 1) during an internal reconnection event (IRE) [14], which increases the elongation. It has been found so far that all high-β shots on START terminate through an IRE. However, an IRE can happen in START at any β value.

Ideal MHD stability analysis shows that the pressure profile in the high-β shots was close to marginal stability

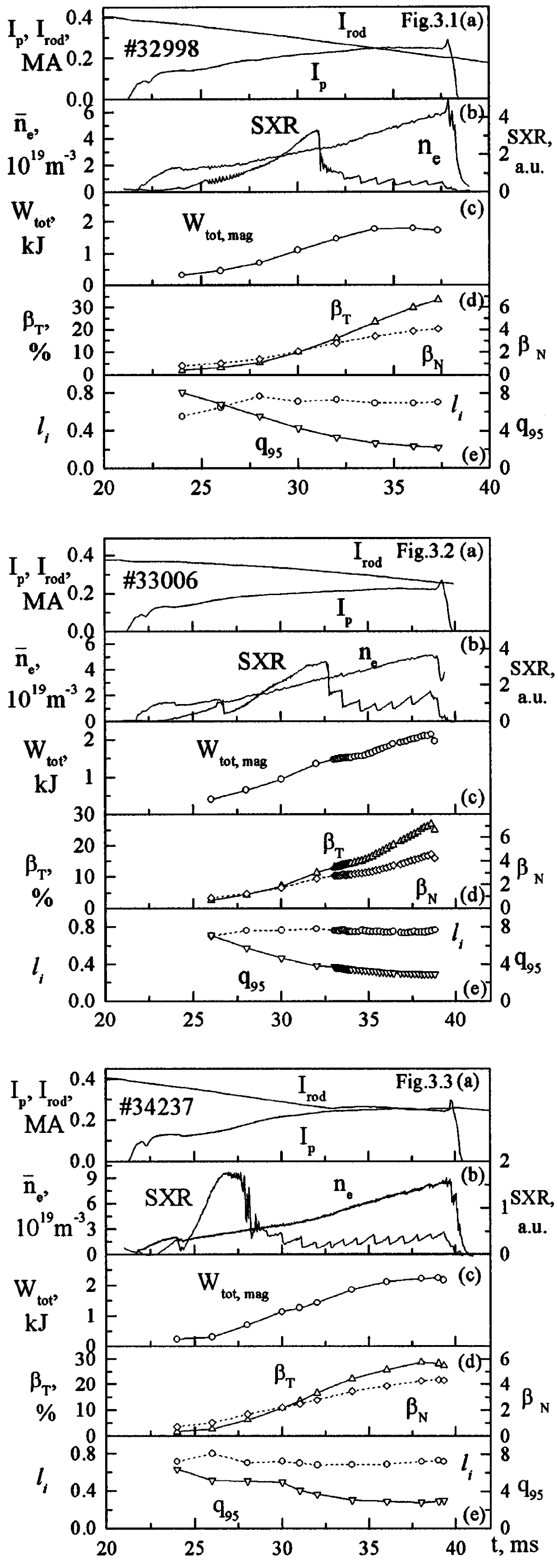

FIG. 3. Wave forms for high-β shots in START, (3.1): #32998; (3.2): #33006; (3.3): #34237. (a) Plasma current, central rod current; (b) line average n_e, soft x-ray (SXR) central chord signal; (c) evolution of total plasma energy; (d),(e) β_T, β_N, l_i, and q_{95} values from equilibrium reconstruction (EFIT).

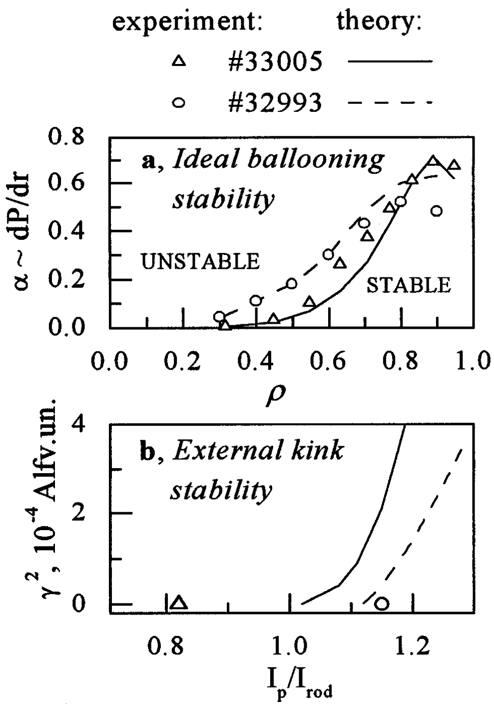

FIG. 5. Ideal ballooning (a) and external kink (b) stability of high-β shots on START. $\rho = [(\psi - \psi_0)/(\psi_{\mathrm{edge}} - \psi_0)]^{0.5}$—radial-like flux variable, γ—growth rate. #33005: $q_{95} = 2.8$, $\beta_T = 23.6\%$, $\beta_N = 4.14$; #32993: $q_{95} = 2.28$, $\beta_T = 30.8\%$, $\beta_N = 3.89$.

to high-n ballooning modes in the first region of stability, Fig. 5(a). Low-n stability calculations (for a limiter equilibrium matching the 95% flux surface position, elongation, and triangularity of the double-null divertor plasma of the experiment) using the ERATO [15] and CHEASE [16] codes show that while the low-q shots were close to instability of external kink modes, Fig. 5(b), the higher-q shots were theoretically stable. In the simulations, both cases become unstable to low-n pressure driven internal modes for pressure profiles more peaked than the experimental value. However, the terminations in the highest β shots appear very similar to those at lower β or higher q. It is thus unclear whether the external kink mode is playing a role in terminating the high-β discharge, although a large helical distortion of the plasma boundary is often seen on the high-speed CCD camera during an IRE at low q. Therefore, despite the proximity to the ideal-MHD kink limit at lower q and to the ballooning limit at high β_N, there is no conclusive experimental evidence that a β limit has been reached on START. Further improvements to START, including a further increase in NBI power, are planned in order to test more fully the predicted β limits.

This work is jointly funded by the U.K. Department of Trade and Industry and Euratom. Shipment of the NBI equipment was funded by the U.S. DOE. We thank the Lausanne group for providing us with a copy of the ERATO code, and General Atomics for supplying EFIT.

*UKAEA/Euratom Fusion Association.

[1] Y-K. M. Peng and D. J. Strickler, Nucl. Fusion **26**, 769 (1986).
[2] R. D. Stambaugh *et al.,* in Proceedings of the 16th International Conference on Fusion Energy, Montreal, Canada, 1996 (to be published) (IAEA F1-CN-64/G1-2, Vienna).
[3] A. Sykes *et al.*, Nucl. Fusion **32**, 694 (1992).
[4] A. Sykes *et al.,* in *Proceedings of the 16th SOFE Conference, Illinois, 1995* (IEEE, New York, 1996), Vol. 2, p. 1442.
[5] F. Troyon *et al.*, Plasma Phys. Controlled Fusion **26**, 209 (1984).
[6] A. Sykes *et al.,* in *Proceedings of the 11th EPS Conference, Aachen, 1983* (European Physical Society, Petit-Lancy, Switzerland, 1983), Part II, p. 363.
[7] E. J. Strait, Phys. Plasmas **1**, 1415 (1994).
[8] E. Lazarus *et al.*, Phys. Fluids B **4**, 11 (1992).
[9] M. J. Walsh *et al.,* in *Proceedings of the 21st EPS Conference, Kiev, 1996* (European Physical Society, Geneva, 1996), Part III, p. 1457; A. Sykes, Phys. Plasmas **4**, 1665 (1997).
[10] M. Mauel *et al., Plasma Physics and Controlled Nuclear Fusion Research* (IAEA, Vienna, 1993), Vol. 1, p. 205.
[11] Y. Kamada *et al.*, Nucl. Fusion **34**, 1605 (1994).
[12] L. L. Lao *et al.*, Nucl. Fusion **25**, 1611 (1985).
[13] M. Tournianski *et al.,* in *Proceedings of the 22nd EPS Conference, Berchtesgaden, 1997* (European Physical Society, Geneva, 1997), Part I, p. 241.
[14] R. J. Buttery *et al.,* in *Proceedings of the 21st EPS Conference, Kiev, 1996* (Ref. [9]), Part I, p. 416.
[15] R. Gruber, Comput. Phys. Commun. **21**, 323 (1981).
[16] H. Lutjens *et al.*, Comput. Phys. Commun. **69**, 242 (1992).